J. Dairy Sci. 106:2642–2650
https://doi.org/10.3168/jds.2022-22716

Cellular proliferation and apoptosis in *Staphylococcus aureus*–infected heifer mammary glands experiencing rapid mammary gland growth

Pari H. Baker,[1] Kellie M. Enger,[1] Sheila K. Jacobi,[2] R. Michael Akers,[3] and Benjamin D. Enger[1]*
[1]Department of Animal Sciences, Ohio Agricultural Research and Development Center, The Ohio State University, Wooster 44691
[2]Department of Animal Sciences, The Ohio State University, Columbus 43210
[3]Department of Dairy Science, Virginia Polytechnic Institute and State University, Blacksburg 24061

ABSTRACT

Intramammary infections in nonlactating mammary glands are common and can occur during periods of rapid mammary epithelial cell (MEC) accumulation, which may ultimately reduce total MEC numbers. Reduced MEC numbers, resulting from impaired MEC proliferation and increased cellular apoptosis, are expected to reduce future milk yields. The objective of this study was to measure the degree of cellular proliferation and apoptosis in the epithelial and stromal compartment of uninfected and *Staphylococcus aureus*–infected mammary glands hormonally induced to grow rapidly. Nonpregnant heifers (n = 8) between 11 and 14 mo of age were administered supraphysiological injections of estradiol and progesterone for 14 d. One mammary gland of each heifer was randomly selected and infused with *Staph. aureus* (CHALL) while another mammary gland was designated as an uninfected control on d 8 of injections. Mammary tissues were collected on the last day of hormonal injections from center and edge parenchymal regions and subject to proliferation assessment via Ki-67 staining and apoptotic assessment via terminal deoxynucleotidyl transferase dUTP nick-end labeling. Differences in cellular proliferation between CHALL and uninfected control quarters were not apparent, but proliferation of MEC was marginally greater in edge parenchyma than in center parenchyma. Coincidently, CHALL quarters experienced a greater percentage of apoptotic MEC and lower percentage of stromal cells undergoing apoptosis than uninfected control quarters. This study also provides the first insight into the mechanisms that allow the mammary fat pad to be replaced by expanding mammary epithelium as edge parenchyma contained a greater percentage of apoptotic stromal cells than center parenchyma. When taken together, these data suggest that *Staph. aureus* intramammary infection impairs mammary epithelial growth through reductions in MEC number and by preventing its expansion into the mammary fat pad. These factors during periods of rapid mammary growth are expected to impair first lactation milk yield.
Key words: mastitis, mammary growth, inflammation

INTRODUCTION

Bovine mastitis, primarily caused by an IMI, continues to be a significant problem in the dairy industry. The consequences of IMI in lactating mammary glands have been previously reviewed and reported to increase milk SCC and increase immune cell infiltration within the mammary tissue while damaging the mammary epithelium (Akers and Nickerson, 2011).

Milk yield is a function of the number of secretory mammary epithelial cells (**MEC**) and their secretory activity (Capuco et al., 2001); reductions in MEC number and decreases in secretory activity would be expected to reduce milk yield. Insults from IMI lead to disruptions in MEC differentiation status through the degradation of organelles important for milk synthesis and secretion, MEC undergoing premature involution, and sloughing of MEC into the alveolar lumen (Akers and Nickerson, 2011). Mammary epithelial cell numbers can also be affected by IMI, as Bayles et al. (1998) reported that *Staphylococcus aureus* challenge of MAC-T cells can induce cellular apoptosis, and Long et al. (2001) reported that acute *Escherichia coli* IMI challenge induces MEC apoptosis in lactating bovine mammary glands.

Nonlactating heifers commonly have IMI during first gestation (Larsen et al., 2021). The prevalence of IMI is highest during the last months of pregnancy (Trinidad et al., 1990b; Fox et al., 1995), which is also when the bovine mammary gland experiences the most pronounced degree of MEC accumulation (Swanson and Poffenbarger, 1979). Based on data in lactating cattle, an IMI during periods of marked MEC accumulation is expected to negatively affect mammary growth. It is important, however, to note that total MEC number is influenced by the temporal dynamics of cellular apop-

Received August 30, 2022.
Accepted November 4, 2022.
*Corresponding author: enger.5@osu.edu

tosis and cellular proliferation. Previous investigations have evaluated the degree of cellular proliferation and apoptosis in involuting dry cow mammary glands (Andreotti et al., 2017) and dry cow mammary glands that were hormonally induced to grow and develop (Enger et al., 2019). Enger et al. (2019) reported a greater number of proliferating cells present in the intralobular stroma of infected quarters relative to uninfected quarters, whereas both Andreotti et al. (2017) and Enger et al. (2019) reported that there were a greater number of apoptotic MEC in infected than uninfected quarters. The greater number of proliferating stromal cells and greater number of apoptotic MEC in infected mammary glands coincide with reports of increased areas of intralobular stroma and reduced tissue area occupied by mammary epithelium (Trinidad et al., 1990a; Enger et al., 2018). We (Baker et al., 2023) recently noted similar observations in mammary glands of nonpregnant heifers that had been hormonally stimulated to grow rapidly, suggesting that changes in stromal cell and epithelial cell proliferation and apoptosis rates are responsible for the changes in mammary tissue architecture, but that had not been evaluated in the previous works. The objective of this study was to delineate the degree of cellular proliferation and apoptosis via immunohistochemistry in rapidly growing mammary glands experiencing *Staph. aureus* IMI. The hypothesis of this study was that IMI would increase the percentage of proliferating stromal cells compared with MEC while concurrently increasing the percentage of MEC undergoing apoptosis.

MATERIALS AND METHODS

Study Design

Archived mammary tissues that were collected from a previous study that had been approved by The Ohio State University Institutional Animal Care and Use Committee (Protocol 2020A00000024) were used for this study (Baker et al., 2023). Briefly, nulligravid Holstein heifers (n = 8) with a mean age and BW of 382 d (SD = 7) and 320 kg (SD = 28), respectively, were administered once-daily supraphysiological injections of estradiol (0.1 mg/kg of BW) and progesterone (0.25 mg/kg of BW) for 14 d to stimulate mammary growth. One mammary gland of each heifer was randomly selected and infused with *Staph. aureus* (**CHALL**) while another mammary gland was designated as an uninfected control (**UNINF**) on d 8 of injections. The CHALL quarters were challenged with 7,000 to 7,900 cfu of the *Staph. aureus* novel strain (Smith et al., 1998). On the last day of hormonal injections (d 14), animals were euthanized, and mammary tissues were collected from experimental quarters. All UNINF quarters (n = 8) remained culture negative throughout the trial, and all CHALL quarters (n = 8) remained infected until tissue collection. Mammary tissues were collected from 2 specific glandular regions within the CHALL and UNINF quarters: mammary epithelium that abuts the mammary fat pad, distal to the teat end (edge parenchyma) and mammary epithelium located slightly above the gland cistern, proximal to the teat end (center parenchyma). Collected mammary tissues were fixed in 10% formalin for 48 h and then transferred to 70% ethanol before being embedded in paraffin.

Immunohistochemical Staining

Ki-67 and p40. A first slide set was created to quantify the percentage of proliferating epithelial, myoepithelial, and stromal cells in the mammary tissues. Cells positively staining for p40 were classified as myoepithelial cells (Parsons et al., 2018; Enger et al., 2019) and subsequently used as a morphological marker to differentiate myoepithelial cells from stroma and epithelial cells. Tissues were sectioned, deparaffinized, and rehydrated as described previously (Baker et al., 2023). Antigens were retrieved by incubating sections in 10 m*M* citrate buffer, pH 6.0, for 30 min at 95°C. Slides were cooled undisturbed to room temperature before being washed in Dulbecco's phosphate-buffered saline (**DPBS**), pH 7.4. A hydrophobic barrier pen (Liquid Blocker, Daido Sangyo Co. Ltd.) was used to separate tissue sections on the same slide to prevent antibody solutions on different sections from mixing. All sections were blocked with CAS Block (Thermo Fisher Scientific) for 30 min. The CAS Block was aspirated from sections, and one section on each slide was covered with 100 μL of a primary antibody mixture while the negative control section received 100 μL of CAS Block. The primary antibody mixture contained a Ki-67 1° antibody (cat # MA5-14520, Thermo Fisher Scientific, 1:200 dilution) and a p40 1° antibody (cat # ab172731, Abcam, 1:50 dilution) suspended in CAS Block. Sections were incubated for 16 h at 4°C.

After incubation, the primary antibody mixture and CAS Block were aspirated, and all sections were washed thrice with DPBS for 5 min. All sections were then incubated with 100 μL of a secondary antibody mixture containing an Alexa Fluor 594 antibody (cat # A-11037, Thermo Fisher Scientific, 1:200 dilution) and an Alexa Fluor 488 antibody (cat # A-21121, Thermo Fisher Scientific, 1:200 dilution) at room temperature for 1 h. The secondary antibody mixture was aspirated and washed with DPBS. Sections were counter-stained with 100 μL of 4′,6-diamidino-2-phenylindole (**DAPI**) for 2 min and subsequently washed with 0.5% Tween

20 (Thermo Fisher) in DPBS. A xylene-soaked cotton applicator was used to remove the hydrophobic barrier pen and slides were covered using ProLong Gold Antifade Mountant (Thermo Fisher).

Terminal Deoxynucleotidyl Transferase dUTP Nick-End Labeling. A second slide set was created to label the 3′-end of fragmented DNA to quantify the percentage of apoptotic epithelial and stromal cells undergoing apoptosis. A commercial kit [Click-iT Plus terminal deoxynucleotidyl transferase dUTP nick-end labeling (**TUNEL**) Assay C10618, Thermo Fisher Scientific] was used according to the manufacturer's protocol specific for formalin-fixed and paraffin-embedded tissue. Sections were counter-stained with 50 μL of DAPI (Thermo Fisher) and incubated for 15 min at room temperature. Sections were washed twice with DPBS, coverslipped using ProLong Gold Antifade Mountant, and cured overnight before imaging.

Image Acquisition and Analysis

Ki-67 and p40. Ki-67- and p40-labeled sections were visualized with an IX81 epifluorescent microscope (Olympus Corporation of the Americas) using a 40× UPlanXApo objective and an X-Cite mini 24 LED light source (Excelitas Technologies). A total of 6 random fields of view were identified and imaged for each tissue section at 400× using the monochrome sensor of a DP80 camera (Olympus Corporation of the Americas). The total area of the 6 images was 0.55 mm^2. Three images were acquired from each random field of view and included (1) DAPI-counter-stained nuclei using a DAPI filter cube, (2) Ki-67–positive-stained nuclei using a Texas Red filter cube, and (3) p40-positive-stained nuclei using a fluorescence isothiocyanate filter cube. Images were overlaid by cellSens Imaging Software, which yielded 192 merged images. Edge parenchyma images were taken near the interface of the mammary fat pad to ensure that points of outward growth were represented, and center parenchyma images were randomly acquired within the section. All cell nuclei within these 3 images were manually identified and differentiated as either positively or negatively stained for Ki-67 to produce a percentage of proliferating epithelial, myoepithelial, and stromal cells from the total of each cell type in the respective tissue regions.

TUNEL. A second examination was conducted to quantify the percentage of apoptotic epithelial and stromal cells within the experimental quarters. Tissue sections were visualized using a 20× UPlanXApo objective on the same IX80 microscope. A total of 3 randomly selected fields of view were imaged at 200× where the total area of the 3 images was 1.24 mm^2. Two images were acquired from each random field of view, 1 of DAPI-counter-stained nuclei using a DAPI filter cube, and 1 containing TUNEL-positive-labeled nuclei using a Texas Red filter cube. Images were merged and yielded 96 images. Edge and center parenchyma images were taken similarly to the previous slide set. All cell nuclei within these acquired images were manually identified and differentiated as either positive or negative TUNEL-labeled cells to produce a percentage of apoptotic epithelial and stromal cells from the total of each cell type in the tissue.

Statistical Analyses

Ki-67 and p40. The percentage of positively labeled Ki-67 nuclei in the epithelial and stromal compartments was calculated by the sum of positively labeled nuclei divided by the sum of all nuclei across the 6 images for each unique heifer, quarter, and region combination. The percentages of Ki-67–positive MEC, myoepithelial cells, and stromal cells were analyzed in 3 separate models. Data were initially analyzed using the GLIMMIX procedure in SAS 9.4 (SAS Institute Inc.), but marked issues with overdispersion could not be corrected after multiple adjustments were tried; it was decided that analysis using PROC MIXED was the most appropriate solution, as assumptions of normal data distribution and homogeneous residuals were satisfied. The percentages of Ki-67–positive cells served as dependent variables in 3 separate models. All models included the fixed effects of quarter treatment (n = 2) and parenchyma region (n = 2) and their interaction. The interactive term of treatment and region was not reported due to nonsignificance ($P \geq 0.40$). Heifer nested within cohort was specified as a random effect in all models. The least squares means ± standard error of the means are reported.

TUNEL. The probability of TUNEL-positive nuclei in the epithelial and stromal compartments was analyzed with PROC GLIMMIX in 2 separate models, using a generalized linear mixed model based on the binomial distribution with a logit link function. The dependent variable was the binary response (number of positive-stained cells/total number of cells), and the fixed and random effects in these models were identical to those for Ki-67 and p40 staining. Overdispersion was assessed and no corrective measures were needed. The least squares means ± standard error of the means are reported.

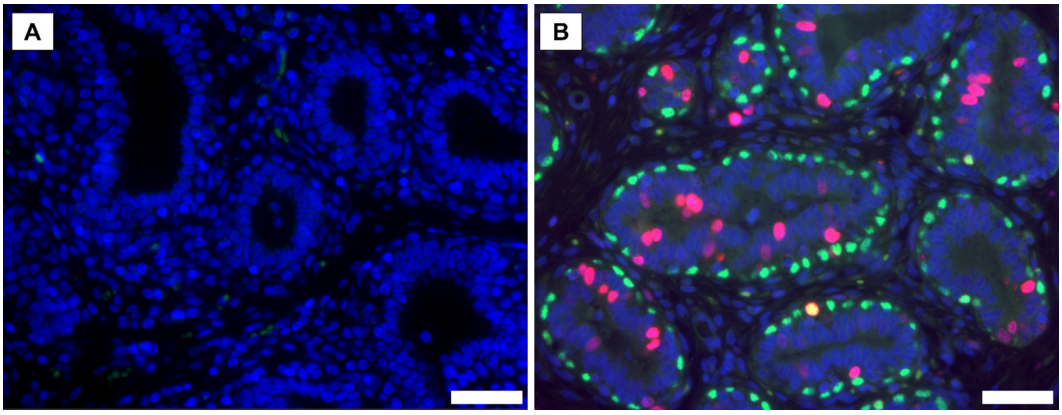

Figure 1. Staining of Ki-67– and p40-positive cell nuclei in mammary tissues. Panel A depicts a negative control section where the primary antibodies (Ki-67 and p40) were omitted; nuclei are counter-stained with 4′,6-diamidino-2-phenylindole (blue). Panel B depicts cells staining positive for Ki-67 (red) and p40 (green) and one proliferating myoepithelial cell staining positive for both Ki-67 and p40 (orange). Scale bar = 20 μm.

RESULTS

Detection of Ki-67–Positive Nuclei

Representative images of Ki-67– and p40-stained mammary tissues are presented in Figure 1, and the percentages of proliferating MEC, myoepithelial cells, and stromal cells for CHALL and UNINF quarters are presented in Figure 2 and Figure 3a. There was no evidence of an interactive effect of quarter treatment and region on the percentage of positive Ki-67 cells for MEC, myoepithelial cells, and stromal cells ($P \geq 0.40$). The percentages of proliferating MEC and myoepithelial cells did not differ between CHALL and UNINF quarters ($P = 0.59$ and $P = 0.95$, respectively). Similarly, the percentage of proliferating stromal cells did not differ between quarter treatments ($P = 0.83$). The percentages of proliferating MEC, myoepithelial cells, and stromal cells within parenchyma region are presented in Figure 3b. There was evidence of a marginally greater ($P = 0.12$) percentage of MEC proliferating in edge parenchyma than center parenchyma (4.5% vs. 3.8% ± 1.3%). For myoepithelial cells and stromal cells, the percentage of proliferating cells did not differ among parenchyma regions ($P = 0.56$ and $P = 0.92$, respectively).

TUNEL

Representative images of TUNEL staining are presented in Figure 2. There was no evidence for an interaction between treatment and region in the epithelial compartment ($P = 0.23$), but the percentage of apoptotic MEC was affected by infection status ($P < 0.0001$). The percentages of apoptotic cells in mammary epithelium and mammary stroma between

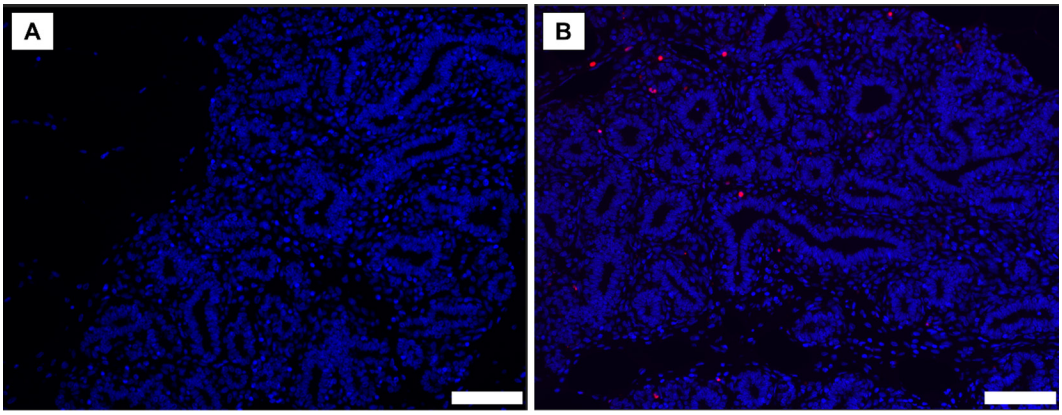

Figure 2. Representative images of apoptosis detection via terminal deoxynucleotidyl transferase dUTP nick-end labeling assay in mammary tissues. Panel A depicts a negative control section. Panel B depicts positive detection of fragmented DNA (red). Scale bar = 50 μm.

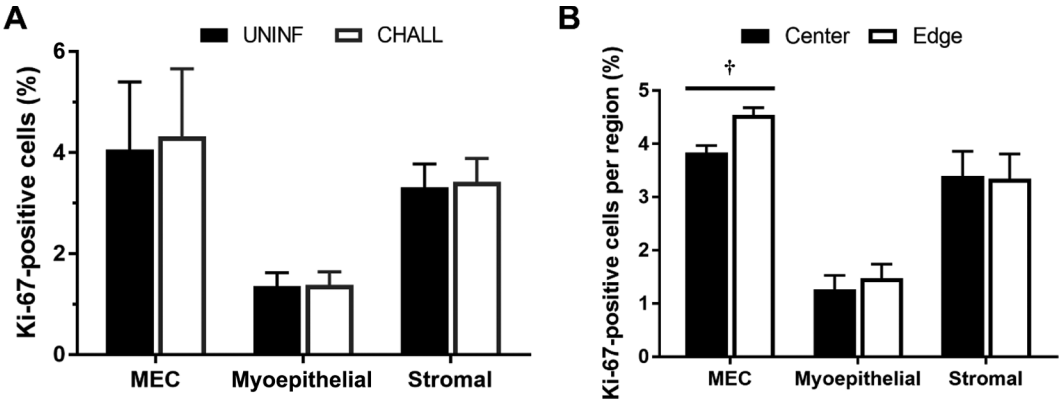

Figure 3. Percentage of proliferating mammary epithelial cells (MEC), myoepithelial cells, and stromal cells by Ki-67 immunostaining. Panel A depicts the percentage of Ki-67–positive cells by treatment, and panel B depicts the percentage of Ki-67–positive cells by region. Values represent the mean ± SEM. †$P = 0.12$. UNINF = uninfected control; CHALL = mammary gland infused with *Staphylococcus aureus*.

quarter treatments are summarized in Figure 4a. The percentage of apoptotic MEC was greater in CHALL quarters relative to UNINF quarters (0.23% ± 0.02% vs. 0.11% ± 0.01%, respectively). The percentage of apoptotic stromal cells was higher in UNINF quarters compared with CHALL quarters (0.38% ± 0.03% vs. 0.25% ± 0.02%; $P = 0.001$). The percentages of apoptotic MEC and stromal cells between edge and center parenchyma are presented in Figure 4b. Differences in MEC apoptotic events were not evident between parenchymal regions ($P = 0.31$), but the percentage of apoptotic stromal cells was marginally greater in edge parenchyma than center parenchyma (0.34% ± 0.02% vs. 0.28% ± 0.03%; $P = 0.06$). There was no evidence for an interactive effect between quarter treatment and region in the stromal compartment ($P = 0.46$).

DISCUSSION

A central objective was to quantify cellular proliferation and contrast proliferation responses in uninfected and *Staph. aureus*–infected mammary glands that had been hormonally stimulated to grow rapidly. We found similar percentages of proliferating MEC in CHALL and UNINF quarters, which agrees with Enger et al. (2019), who also found no difference in MEC proliferation between infected and uninfected mammary glands. Conversely, this observation does not agree with observations by Long et al. (2001) and Andreotti et al. (2017), who reported greater MEC proliferation in infected than uninfected mammary glands. Increased cellular proliferation is anticipated to compensate for cell loss and tissue rearrangement during inflammation

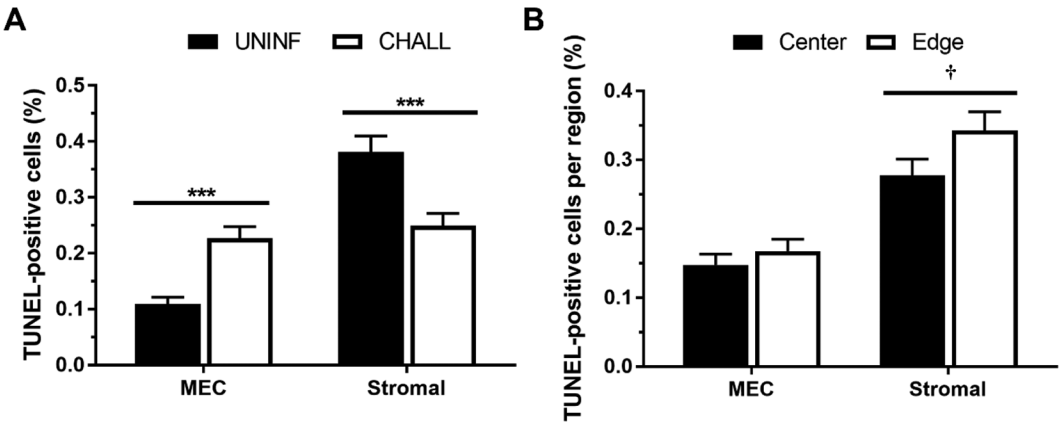

Figure 4. Percentage of apoptotic mammary epithelial cells (MEC) and stromal cells by terminal deoxynucleotidyl transferase dUTP nick-end labeling (TUNEL) immunostaining. Panel A depicts the percentage of TUNEL-positive MEC and stromal cells by treatment, and panel B depicts the percentage of TUNEL-positive cells by region. Values represent the mean ± SEM. Symbols represent statistically significant differences between treatments (†$P < 0.10$, ***$P < 0.001$). UNINF = uninfected control; CHALL = mammary gland infused with *Staphylococcus aureus*.

(Gurtner et al., 2008). Our contrasting results may be a function of the different physiological states of the mammary tissues in the respective studies. Long et al. (2001) evaluated lactating mammary tissue, and Andreotti et al. (2017) studied mammary tissue from actively involuting mammary glands. The tissues examined here were from nonlactating mammary glands that were hormonally stimulated to grow rapidly. No net mammary growth is expected during lactation or early mammary gland involution, as the rate of cellular apoptosis surpasses the rate of cellular proliferation, resulting in a gradual decrease in the total number of MEC (Capuco et al., 2001; Sørensen et al., 2006). On the contrary, mammary tissues obtained from this investigation were rapidly growing due to the mitogenic effect of estradiol (Woodward et al., 1993; Capuco et al., 2002), as evidenced by MEC proliferation percentages exceeding 4% in our tissues relative to 0.3% reported for lactating mammary glands (Capuco et al., 2001). Even if wound repair mechanisms were occurring in the CHALL quarters through compensatory cellular proliferation, an additive effect may not be detectable with the continued administration of hormone injections. Additionally, differences in cellular proliferation may also be caused by severity and duration of inflammation. Long et al. (2001) challenged lactating mammary glands with *Escherichia coli*, which generally causes more acute clinical mastitis than *Staph. aureus* and more extensive tissue damage and even death (Burvenich et al., 2003; Bannerman et al., 2004). Andreotti et al. (2017) examined involuting mammary glands with chronic, naturally acquired *Staph. aureus* IMI during the previous dry period or early lactation, resulting in a considerably longer infection, whereas the mammary tissues examined by us were obtained only 6 d post–*Staph. aureus* challenge. Regardless, when mammary tissues in the present study were examined previously (Baker et al., 2023), less tissue area was occupied by mammary epithelium in CHALL quarters, indicating that factors other than cellular proliferation contributed to the reduced areas of mammary epithelium. In addition, differences in epithelial tissue area likely reflect the consequences of changes in cell proliferation occurring over a prolonged period of time. Measurement of the percentage of proliferating MEC reflects the state of the tissue during the hours just before tissue sample collection.

The percentage of proliferating MEC was only marginally greater in edge parenchyma than center parenchyma (4.5% vs 3.8%, respectively). This observation somewhat aligns with previous reports detailing greater epithelial cell proliferation in outer parenchyma than centrally located parenchyma (Capuco et al., 2002; Hardy et al., 2021), but the studies of Capuco et al. and Hardy et al. evaluated prepubertal heifer mammary glands. Interestingly, the disparity in MEC proliferation existing between center and edge mammary parenchyma was not as pronounced as in the previous reports, approximately 5.5% versus 11.3% for Capuco et al. (2002) and 2.3% versus 10.8% for Hardy et al. (2021), respectively. It seems likely that this difference arises from differences in mammary gland physiology. In 3-mo-old prepubertal heifers, the mammary epithelium is present as a dense mass immediately above the teat. The separation between the epithelium and fat pad is acute, with scant indications of epithelial branching into the fat pad matrix, which occupies the greatest volume of the mammary gland. The epithelium rapidly grows during 4 to 9 m of age (Sinha and Tucker, 1969) and infiltrates the mammary fat in a branching manner. The dramatic differences in proliferation between edge and center parenchyma in prepubertal heifers are expected, as these animals are experiencing extensive epithelial outgrowth into the fat pad for the first time. On the contrary, mammary gland growth was hormonally stimulated in our study, and these mammary glands were from breeding-age heifers between the ages of 11 and 14 mo old. Therefore, parenchymal regions would appear relatively homogeneous as significant epithelial branching of mammary ducts into the mammary fat has already occurred in these regions.

Concerning the degree of myoepithelial cell proliferation, percentages did not differ between quarter treatments or parenchyma region. The lack of disparity may be a result of the hormone induction protocol, as it has been previously reported that ovarian secretions stimulate epithelial proliferation and block myoepithelial differentiation (Ballagh et al., 2008; Safayi et al., 2012). The supraphysiological administration of estradiol and progesterone here may have affected myoepithelial cell proliferation and differentiation. Additionally, aside from their well-characterized role in milk ejection, myoepithelial cells are also associated with gland morphogenesis and establishing cell polarity (Gudjonsson et al., 2005) and have been implicated in tumor suppression in humans (Adriance et al., 2005). The role of myoepithelial cells during IMI remains unknown, but Enger et al. (2019) previously reported that the nuclear area of p40 staining was significantly greater in *Staph. aureus*–infected quarters. Whether myoepithelial cells play a significant role during postpubertal mammary growth or during IMI warrants future investigations.

The lack of difference in cellular proliferation within the stromal compartment between quarter treatments does not align with previous reports (Long et al., 2001; Andreotti et al., 2017; Enger et al., 2019). Stromal cells, predominantly composed of fibroblasts, can influence the inflammatory response by regulating MEC function

and altering the initiation, development, and resolution of inflammation (Chen et al., 2016). We posit that the lack of difference in stromal cell proliferation arises from differences in IMI severity and duration, as well as the unique physiological state of our examined mammary glands. The inflammation present in our examined tissues may not have been severe enough to elicit changes in stromal cell proliferation given that no clinical signs of disease were observed, differing from previous reports (Long et al., 2001; Enger et al., 2018). The scant accumulation of mammary secretions, coupled with the fact that prepartum secretions have minimal concentrations of lactose (Akers, 2002), is expected to limit bacterial growth, which may have diminished the heifer's response to IMI. Additionally, with these mammary tissues undergoing induced mammary growth via supraphysiological injections of estradiol and progesterone, any potential differences in stromal cell proliferation may be undetectable as a result of the hormone induction protocol. We (Baker et al., 2023) recently reported similar observations regarding greater tissue area occupied by intralobular stroma in CHALL quarters relative to UNINF quarters, but these tissue changes were not reflected in the changes in rates of cell proliferation measured on the day of tissue collection.

Between parenchyma regions, stromal cell proliferation did not differ. To our knowledge, this is the first study to investigate the degree of stromal cell proliferation between edge and center regions of the mammary gland. Our results suggest that the lack of stromal cell proliferation in both areas allows for the mammary epithelium to continue to expand into the mammary fat pad. This conjecture coincides with the marginally greater degree of MEC proliferation occurring in edge parenchyma than center parenchyma in these mammary tissues. Continued investigations to ascertain patterns of stromal cell proliferation between regions of the mammary gland during distinct physiological periods should be considered.

The second objective was to delineate the degree of cellular apoptosis in the epithelial and stromal compartments in CHALL and UNINF mammary tissues. As expected, CHALL quarters experienced a greater degree of MEC apoptosis than UNINF quarters, which is consistent with previous reports (Long et al., 2001; Andreotti et al., 2017; Enger et al., 2019). It has been documented previously that *Staph. aureus* can damage mammary epithelium by inducing necrosis of secretory tissues (Chandler and Reid, 1973) and replacing secretory tissue with nonsecretory tissue in both lactating cows (Nickerson and Heald, 1981) and nonpregnant dairy heifers (Trinidad et al., 1990b). Additionally, the ability of *Staph. aureus* to induce cell death has been demonstrated in challenged MAC-T cells (Bayles et al., 1998); *Escherichia coli* challenge of lactating mammary glands in vivo has been similarly documented to induce MEC apoptosis (Long et al., 2001). Mammary tissue damage may also be attributed to the recruitment and activation of neutrophils and other leukocytes from the blood to the site of infection. Neutrophils can inadvertently damage MEC via release of enzymes and reactive oxygen species that can induce swelling of secretory epithelial cytoplasm and sloughing of MEC and reduce their secretory activity (Paape et al., 2002; Zhao and Lacasse, 2008). The greater percentage of MEC undergoing apoptosis in CHALL quarters is speculated to be a result of the direct effects of *Staph. aureus* and its associated inflammatory response. Additionally, the greater degree of MEC apoptosis aligns with the reductions in mammary epithelial tissue area observed previously (Baker et al., 2023). Overall, there appears to be an impairment in the accumulation of MEC in CHALL quarters.

How the bovine mammary fat pad complements the advancement of the epithelium has been unclear, and this study provides the first insight into the cellular dynamics that allows the mammary fat pad to be replaced by expanding mammary epithelium. Our results suggest mammary epithelial expansion is complemented by stromal cell apoptosis. Edge parenchyma, where mammary epithelium is invading the mammary fat pad, contained a greater percentage of apoptotic stromal cells compared with center parenchyma. Although both edge and center parenchyma experienced a marginal difference in stromal cell proliferation, the rate of cellular apoptosis in edge parenchyma was about 20% higher than in center parenchyma, allowing for the mammary fat pad to regress at a faster rate in the outer region. This stromal regression would allow for the expanding mammary epithelium to replace the previously existing mammary fat pad or stromal in these rapidly growing mammary glands. However, continued investigations into the mechanisms that allow for the mammary epithelium to replace the stromal fat pad matrix during periods of mammary growth are warranted.

The result that CHALL quarters contained a lower percentage of apoptotic stromal cells than UNINF quarters coincides with the marginally greater tissue area occupied by intralobular stroma in CHALL quarters relative to UNINF quarters in our earlier report (Baker et al., 2023). This observation indicates that intralobular stroma fails to regress in CHALL quarters at a rate comparable to that in UNINF quarters, preventing the expansion of the mammary epithelium into the fat pad. From our results, greater apoptosis within the stromal compartment in UNINF quarters is an important mechanism for the regression of intralobular

stroma during periods of rapid mammary growth. The mammary fat pad in ruminants is extensively interlaced with a network of fibroblasts and associated connective tissue fibrils separating it into rope-like cords (Hovey et al., 1999). Moreover, these connective tissue cords have been speculated to direct parenchymal outgrowth (Hovey et al., 1999). With this in observation, it would suggest that as the mammary epithelium grows in the direction of the septa, components of the mammary fat pad are degraded to allow for the continued replacement of mammary epithelium. Overall, these underlined dynamics of cellular proliferation and apoptosis between parenchyma regions provide greater clarity regarding postpubertal mammary growth and development.

CONCLUSIONS

Mammary gland growth depends on a dynamic interaction between cellular proliferation and apoptosis. Imbalances between the rate of proliferation and apoptosis would either increase the number of cells within the mammary gland or reduce their number. Results indicate that IMI reduced the rate of MEC proliferation while reducing the rate of stromal cell apoptosis, suggesting that IMI impairs mammary epithelial growth over time. These results coincide with the decrease in mammary epithelial tissue area and increase in intralobular stroma tissue area observed previously (Baker et al., 2023). Additionally, this investigation provides the first evidence of potential cellular mechanisms that facilitate the replacement of the bovine mammary fat pad by the epithelium during acute mammary gland growth. Overall, these data suggest that *Staph. aureus* IMI impairs the rate of MEC accumulation and its expansion into the mammary fat pad while reducing stromal cell regression during periods of rapid mammary gland growth. These factors together are expected to impair future milk yield and reduce herd productivity, highlighting the importance of managing and preventing IMI in heifers.

ACKNOWLEDGMENTS

This work was supported by a competitive grant funded by USDA NIFA (Washington, DC) awarded to B. D. Enger (grant no. 2020-67015-31677). The authors have not stated any conflicts of interest.

REFERENCES

Adriance, M. C., J. L. Inman, O. W. Petersen, and M. J. Bissell. 2005. Myoepithelial cells: Good fences make good neighbors. Breast Cancer Res. 7:190. https://doi.org/10.1186/bcr1286.

Akers, R. M. 2002. Overview of mammary development. Pages 8–32 in Lactation and the Mammary Gland. 1st ed. Blackwell Publishing Company.

Akers, R. M., and S. C. Nickerson. 2011. Mastitis and its impact on structure and function in the ruminant mammary gland. J. Mammary Gland Biol. Neoplasia 16:275–289. https://doi.org/10.1007/s10911-011-9231-3.

Andreotti, C. S., E. A. L. Pereyra, S. C. Sacco, C. Baravalle, M. S. Renna, H. H. Ortega, L. F. Calvinho, and B. E. Dallard. 2017. Proliferation-apoptosis balance in *Staphylococcus aureus* chronically infected bovine mammary glands during involution. J. Dairy Res. 84:181–189. https://doi.org/10.1017/S002202991700005X.

Baker, P. H., S. K. Jacobi, R. M. Akers, and B. D. Enger. 2023. Histological tissue structure alterations resulting from *Staphylococcus aureus* intramammary infection in heifer mammary glands hormonally induced to rapidly grow and develop. J. Dairy Sci. 106:1370–1382. https://doi.org/10.3168/jds.2022-22463.

Ballagh, K., N. Korn, L. Riggs, S. L. Pratt, F. Dessauge, R. M. Akers, and S. Ellis. 2008. Hot topic: Prepubertal ovariectomy alters the development of myoepithelial cells in the bovine mammary gland. J. Dairy Sci. 91:2992–2995. https://doi.org/10.3168/jds.2008-1191.

Bannerman, D. D., M. J. Paape, J. W. Lee, X. Zhao, J. C. Hope, and P. Rainard. 2004. *Escherichia* coli and *Staphylococcus aureus* elicit differential innate immune responses following intramammary infection. Clin. Vaccine Immunol. 11:463–472. https://doi.org/10.1128/CDLI.11.3.463-472.2004.

Bayles, K. W., C. A. Wesson, L. E. Liou, L. K. Fox, G. A. Bohach, and W. R. Trumble. 1998. Intracellular *Staphylococcus aureus* escapes the endosome and induces apoptosis in epithelial cells. Infect. Immun. 66:336–342. https://doi.org/10.1128/IAI.66.1.336-342.1998.

Burvenich, C., V. R. Van Merris, J. Mehrzad, A. Diez-Fraile, and L. Duchateau. 2003. Severity of *E. coli* mastitis is mainly determined by cow factors. Vet. Res. 34:521–564. https://doi.org/10.1051/vetres:2003023.

Capuco, A. V., S. Ellis, D. L. Wood, R. M. Akers, and W. Garrett. 2002. Postnatal mammary ductal growth: Three-dimensional imaging of cell proliferation, effects of estrogen treatment, and expression of steroid receptors in prepubertal calves. Tissue Cell 34:143–154. https://doi.org/10.1016/S0040-8166(02)00024-1.

Capuco, A. V., D. L. Wood, R. Baldwin, K. McLeod, and M. J. Paape. 2001. Mammary cell number, proliferation, and apoptosis during a bovine lactation: Relation to milk production and effect of bST. J. Dairy Sci. 84:2177–2187. https://doi.org/10.3168/jds.S0022-0302(01)74664-4.

Chandler, R. L., and I. M. Reid. 1973. Ultrastructural and associated observations on clinical cases of mastitis in cattle. J. Comp. Pathol. 83:233–241. https://doi.org/10.1016/0021-9975(73)90047-9.

Chen, Q., G. He, W. Zhang, T. Xu, H. Qi, J. Li, Y. Zhang, and M.-Q. Gao. 2016. Stromal fibroblasts derived from mammary gland of bovine with mastitis display inflammation-specific changes. Sci. Rep. 6:27462. https://doi.org/10.1038/srep27462.

Enger, B. D., C. E. Crutchfield, T. T. Yohe, K. M. Enger, S. C. Nickerson, C. L. M. Parsons, and R. M. Akers. 2018. *Staphylococcus aureus* intramammary challenge in non-lactating mammary glands stimulated to rapidly grow and develop with estradiol and progesterone. Vet. Res. 49:47. https://doi.org/10.1186/s13567-018-0542-x.

Enger, B. D., S. N. Lehner, C. L. M. Parsons, R. M. Akers, and N. R. Hardy. 2020. Effects of intramammary infection and parenchymal region on collagen abundance in nonlactating bovine mammary glands. Appl. Anim. Sci. 36:688–693. https://doi.org/10.15232/aas.2020-02003.

Enger, B. D., S. C. Nickerson, H. L. M. Tucker, C. L. M. Parsons, and R. M. Akers. 2019. Apoptosis and proliferation in *Staphylococcus aureus*-challenged, nonlactating mammary glands stimulated to grow rapidly and develop with estradiol and progesterone. J. Dairy Sci. 102:857–865. https://doi.org/10.3168/jds.2018-15498.

Fox, L. K., S. T. Chester, J. W. Hallberg, S. C. Nickerson, J. W. Pankey, and L. D. Weaver. 1995. Survey of intramammary infections in dairy heifers at breeding age and first parturition. J. Dairy Sci.

78:1619–1628. https://doi.org/10.3168/jds.S0022-0302(95)76786-8.

Gudjonsson, T., M. C. Adriance, M. D. Sternlicht, O. W. Petersen, and M. J. Bissell. 2005. Myoepithelial cells: Their origin and function in breast morphogenesis and neoplasia. J. Mammary Gland Biol. Neoplasia 10:261–272. https://doi.org/10.1007/s10911-005-9586-4.

Gurtner, G. C., S. Werner, Y. Barrandon, and M. T. Longaker. 2008. Wound repair and regeneration. Nature 453:314–321. https://doi.org/10.1038/nature07039.

Hardy, N. R., K. M. Enger, J. Hanson, M. L. Eastridge, L. E. Moraes, and B. D. Enger. 2021. Organization of mammary blood vessels as affected by mammary parenchymal region and estradiol administration in Holstein heifer calves. J. Dairy Sci. 104:6200–6211. https://doi.org/10.3168/jds.2020-19233.

Hovey, R. C., T. B. McFadden, and R. M. Akers. 1999. Regulation of mammary gland growth and morphogenesis by the mammary fat pad: A species comparison. J. Mammary Gland Biol. Neoplasia 4:53–68. https://doi.org/10.1023/A:1018704603426.

Larsen, L. R., P. H. Baker, K. M. Enger, L. E. Moraes, P. R. F. Adkins, J. A. Pempek, C. A. Zimmerly, S. M. Gauta, R. L. Bond, and B. D. Enger. 2021. Administration of internal teat sealant in primigravid dairy heifers at different times of gestation to prevent intramammary infections at calving. J. Dairy Sci. 104:12773–12784. https://doi.org/10.3168/jds.2021-20819.

Long, E., A. V. Capuco, D. L. Wood, T. Sonstegard, G. Tomita, M. J. Paape, and X. Zhao. 2001. *Escherichia coli* induces apoptosis and proliferation of mammary cells. Cell Death Differ. 8:808–816. https://doi.org/10.1038/sj.cdd.4400878.

Nickerson, S. C., and C. W. Heald. 1981. Histopathologic response of the bovine mammary gland to experimentally induced *Staphylococcus aureus* infection. Am. J. Vet. Res. 42:1351–1355.

Paape, M. J., K. Shafer-Weaver, A. V. Capuco, K. Van Oostveldt, and C. Burvenich. 2002. Immune surveillance of mammary tissue by phagocytic cells. Pages 259–277 in Biology of the Mammary Gland: Advances in Experimental Medicine and Biology. J. A. Mol and R. A. Clegg, ed. Springer US.

Parsons, C. L. M., H. L. M. Tucker, R. M. Akers, and K. M. Daniels. 2018. Technical note: p40 antibody as a replacement for p63 antibody in bovine mammary immunohistochemistry. J. Dairy Sci. 101:7614–7617. https://doi.org/10.3168/jds.2018-14676.

Safayi, S., N. Korn, A. Bertram, R. M. Akers, A. V. Capuco, S. L. Pratt, and S. Ellis. 2012. Myoepithelial cell differentiation markers in prepubertal bovine mammary gland: Effect of ovariectomy. J. Dairy Sci. 95:2965–2976. https://doi.org/10.3168/jds.2011-4690.

Sinha, Y. N., and H. A. Tucker. 1969. Mammary development and pituitary prolactin level of heifers from birth through puberty and during the estrous cycle. J. Dairy Sci. 52:507–512. https://doi.org/10.3168/jds.S0022-0302(69)86595-1.

Smith, T. H., L. K. Fox, and J. R. Middleton. 1998. Outbreak of mastitis caused by one strain of *Staphylococcus aureus* in a closed dairy herd. J. Am. Vet. Med. Assoc. 212:553–556.

Sørensen, M. T., J. V. Nørgaard, P. K. Theil, M. Vestergaard, and K. Sejrsen. 2006. Cell turnover and activity in mammary tissue during lactation and the dry period in dairy cows. J. Dairy Sci. 89:4632–4639. https://doi.org/10.3168/jds.S0022-0302(06)72513-9.

Swanson, E. W., and J. I. Poffenbarger. 1979. Mammary gland development of dairy heifers during their first gestation. J. Dairy Sci. 62:702–714. https://doi.org/10.3168/jds.S0022-0302(79)83313-5.

Trinidad, P., S. C. Nickerson, and R. W. Adkinson. 1990a. Histopathology of staphylococcal mastitis in unbred dairy heifers. J. Dairy Sci. 73:639–647. https://doi.org/10.3168/jds.S0022-0302(90)78715-2.

Trinidad, P., S. C. Nickerson, and T. K. Alley. 1990b. Prevalence of intramammary infection and teat canal colonization in unbred and primigravid dairy heifers. J. Dairy Sci. 73:107–114. https://doi.org/10.3168/jds.S0022-0302(90)78652-3.

Woodward, T. L., W. E. Beal, and R. M. Akers. 1993. Cell interactions in initiation of mammary epithelial proliferation by oestradiol and progesterone in prepubertal heifers. J. Endocrinol. 136:149–157. https://doi.org/10.1677/joe.0.1360149.

Zhao, X., and P. Lacasse. 2008. Mammary tissue damage during bovine mastitis: Causes and control. J. Anim. Sci. 86(suppl_13):57–65. https://doi.org/10.2527/jas.2007-0302.

ORCIDS

Pari H. Baker https://orcid.org/0000-0003-4943-9279
Kellie M. Enger https://orcid.org/0000-0002-8295-4128
Sheila K. Jacobi https://orcid.org/0000-0002-2374-2280
R. Michael Akers https://orcid.org/0000-0002-0840-2253
Benjamin D. Enger https://orcid.org/0000-0001-7760-3107